OPEN JOURNAL SYSTEMS
ISSN:2237-2202

Available on line at Directory of Open Access Journals
Journal of Hyperspectral Remote Sensing v12., n03. (2022) 124-130.

www.periodicos.ufpe.br/revistas/jhrs

Journal of Hyperspectral Remote Sensing
www.ufpe.br/jhrs

Prospection for economic mineralization using PRISMA satellite hyperspectral remote sensing imagery: an example from central East Greenland

Enton Bedini* and Jiang Chen**

*International Institute of Geoinformation Science and Earth Observation (ITC), Enschede, The Netherlands. Email: enton_bedini@hotmail.com. (Corresponding author).

**Shenyang Institute of Geology and Mineral Resources, CGS, Shenyang, Liaoning, 110034, China. Email: chen07761@itc.nl

Received 01/06/2022; accepted 08/24/2022.

ABSTRACT

The PRISMA hyperspectral imaging satellite of the Italian Space Agency records in the 0.4-2.5 μm wavelength region at a spatial resolution of 30 m. This study used the PRISMA hyperspectral imagery to characterize an extensive hydrothermal alteration system in the Kap Simpson igneous complex in central East Greenland. The prospection for economic mineralization in the study area has been in the focus of the activities of several mineral exploration companies. The PRISMA data were analyzed using the Adaptive Coherence Estimator. The hyperspectral imagery mapped the spatial distribution of several alteration minerals. The hyperspectral data identified widespread iron stained zones consisting of limonite and jarosite. All these zones constitute prospection targets for the localization of economic mineralization of molybdenum, rare earth elements, gold, silver, and base metals. The study indicates the applicability of PRISMA imagery for the prospection of economic mineralization. The results should also be useful for the evaluation of the PRISMA hyperspectral imagery in geoenvironmental applications.

Keywords: hyperspectral, satellite, PRISMA, reflectance spectroscopy, economic mineralization

Introduction

The PRISMA (Hyperspectral Precursor of the Application Mission) hyperspectral imaging satellite of the Italian Space Agency is a pushbroom sensor that records in the 0.4-2.5 μm wavelength region (Heller Pearlshtien et al., 2021; Bedini and Chen, 2020; Pignatti et al., 2013). The PRISMA hyperspectral data have a spatial resolution of 30 m. The PRISMA satellite hyperspectral data are used in environmental monitoring, agriculture, forest and grassland mapping, land use and land cover mapping, hydrology, glaciology etc. The visible to short wave infrared (0.4-2.5 μm) region of the electromagnetic spectrum is also useful for the remote sensing of natural resources (e.g. van der Meer et al., 2012; Bedini, 2017; and references therein).

An extensive hydrothermal alteration system is exposed in central East Greenland in the area of Kap Simpson (figure 1, Conradsen and Harpøth, 1984). The Kap Simpson igneous complex has been in the focus of the activities of several mineral exploration companies (Geyti, 1979; Damtoft and Grahl-Madsen, 1982; CGRG, 2012; among others). Lithogeochemical data have indicated high anomalous values of molybdenum, and rare earth elements. The alteration in the area has also been investigated by the analysis of Landsat imagery (Conradsen and Harpøth, 1984), Advanced Spaceborne Thermal Emission and Reflection Radiometer (ASTER) data, and airborne hyperspectral imagery (Bedini, 2011).

This paper reports on the application of the PRISMA satellite imagery for the characterization of the hydrothermal alteration in this area of East Greenland. The analysis of PRISMA hyperspectral data could be useful to guide field activities in the area for the prospection of molybdenum, rare earth elements, lead and zinc, gold and silver resources. The results should also be useful for the evaluation of the PRISMA satellite hyperspectral imagery in geoenvironmental applications.

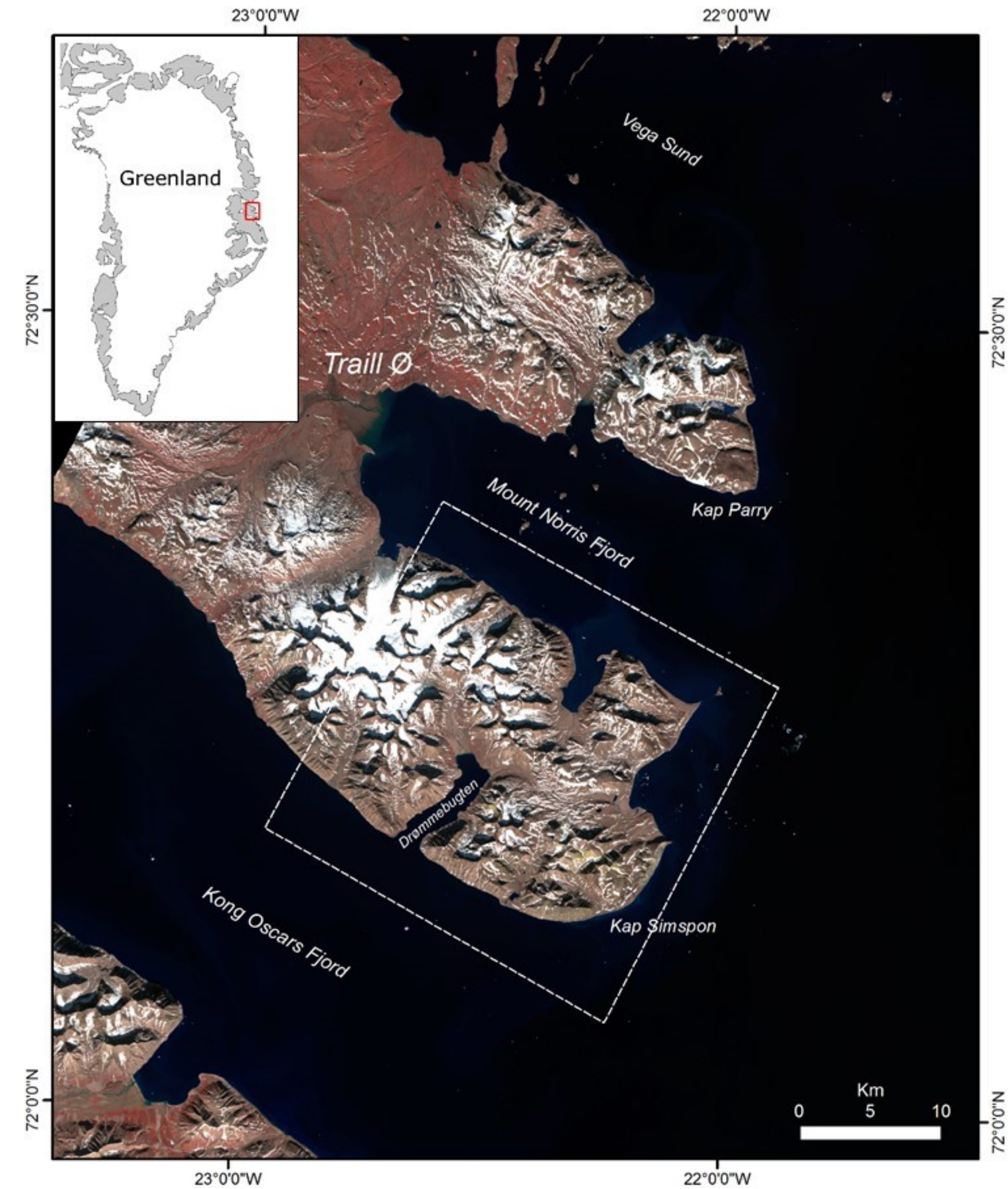

Figure 1. The study area in central East Greenland (indicated by the white dashed-line rectangle) shown on a Landsat color-infrared composite image.

Materials and methods

Study area

The Paleogene intrusions and magmatic complexes emplaced in East Greenland host a range of economic mineralization (Harpøth et al., 1986; Tukiainen and Thomassen, 2010). The Kap Simpson igneous rocks complex occurs in central East Greenland. The eastern part of the Kap Simpson igneous rocks complex is composed of a caldera with extensive hydrothermal alteration including silicification, argillization and pyritization. The alteration includes large areas of iron oxide staining with spectacular colour anomalies visible on the surface (figure 2). The area has been explored for porphyry molybdenum deposits, fluorite, rare earth elements, gold, silver etc., by geochemistry of stream sediments and lithogeochemistry (e.g., Harpøth et al., 1986). Molybdenum mineralization has been found at several localities, but the size and grade are insignificant (Harpøth et al., 1986).

The PRISMA hyperspectral imagery of the Kap Simpson study area (figure 3) was recorded on July 27, 2021. The PRISMA apparent surface reflectance data (L2D) have been shown comparable to airborne hyperspectral data (Bedini and Chen, 2020; Heller Pearlshtien et al., 2021). In order to have a full coverage of the study area subsets of two PRISMA scenes were merged. A strip of no-data occurs between two consecutive PRISMA scenes. The georeferencing accuracy of the hyperspectral scenes was improved by using ground control points from topographic maps.

The spectral reflectance properties of the altered rocks

Reflectance spectra in the 0.4-2.5 µm wavelength range of altered rock samples from the Kap Simpson complex were recorded using an Analytical Spectral Device (ASD). The visible to short wave infrared-active alteration mineralogy in the reflectance spectra of these samples consists mainly of limonite, jarosite, illite and kaolinite. The reflectance spectra of the altered rocks from the Kap Simpson complex display absorption features due to electronic processes involving Fe^{3+}, and to molecular vibrational processes in OH^- bearing minerals (figure 4; Bedini, 2011; Bishop and Murad, 2005). The mineral jarosite has a broad ferric iron absorption feature near 0.90 µm, is more reflective overall than limonite and displays a local reflectance maximum at near 0.70 µm. Jarosite has also vibrational absorption features due to Fe-OH and OH stretches and bending (Bishop and Murad, 2005). Limonite (goethite) has characteristic absorption features in the visible to near infrared wavelength region due to electronic transitions of ferric iron (Clark, 1999). Limonite displays a broad ferric iron absorption feature near 0.90 µm, and two additional features near 0.50 µm and 0.66 µm with a peak near 0.75 µm (Clark, 1999). The reflectance spectrum of illite displays an intense Al-OH absorption feature near 2.20 µm, whereas the reflectance spectrum of kaolinite displays an Al-OH doublet absorption feature at around 2-17-2.20 µm (Clark, 1999).

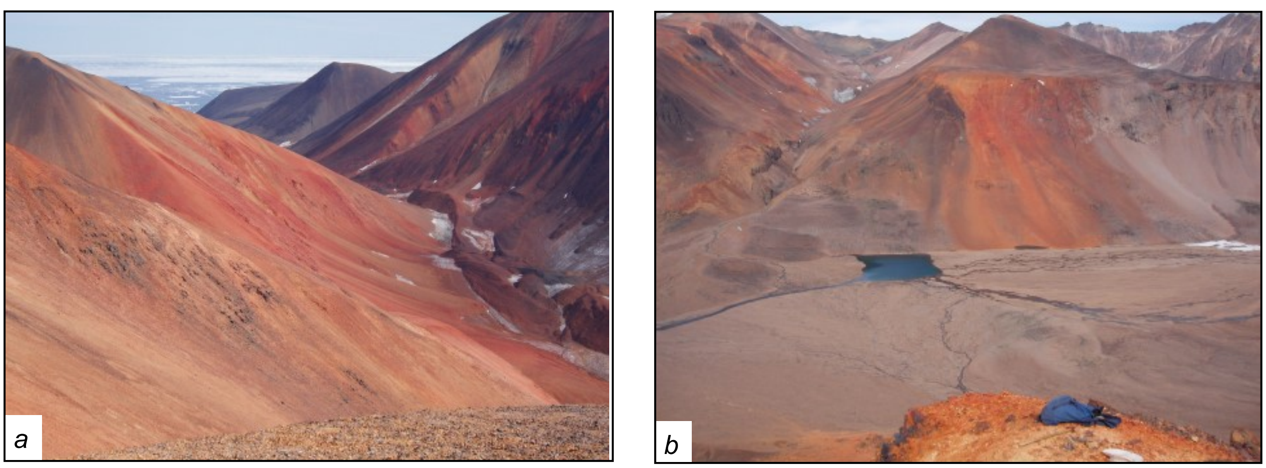

Figure 2. Extensive iron stained zones in the Kap Simpson complex. (a) Føndal. Relief is ca. 400 m. (b) in the western side of Forårsdal. Relief is ca. 500 m. (Field photographs courtesy of Bjørn Thomassen, Geological Survey of Denmark and Greenland).

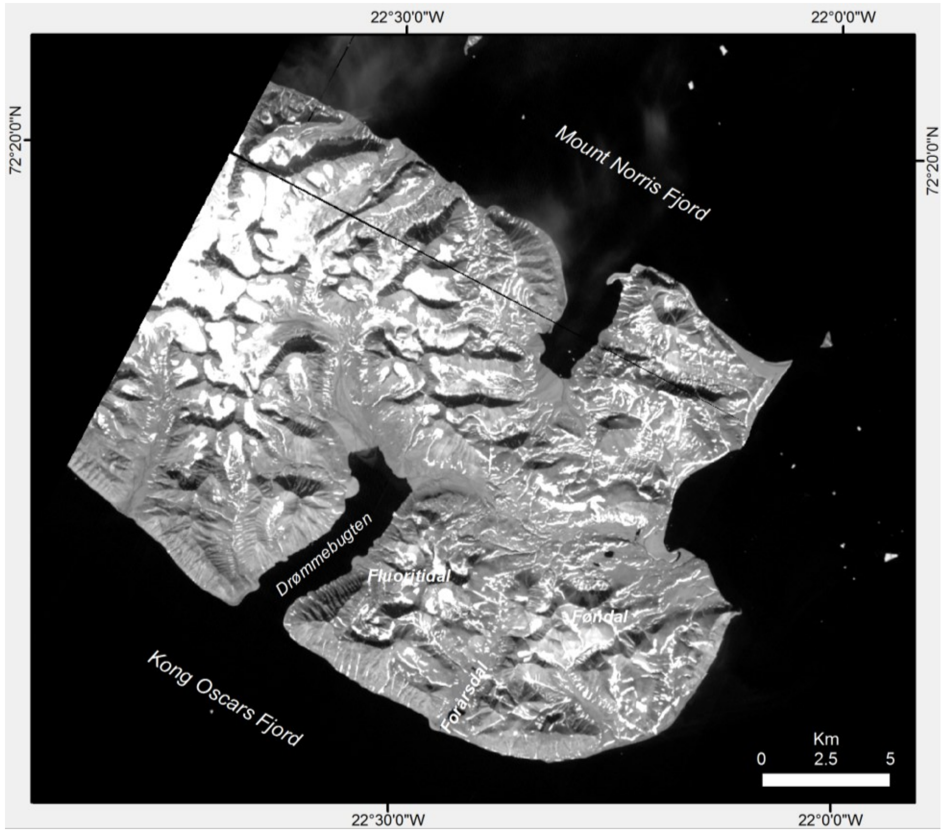

Figure 3. The Kap Simpson PRISMA image (band 32 = 0.65 μm).

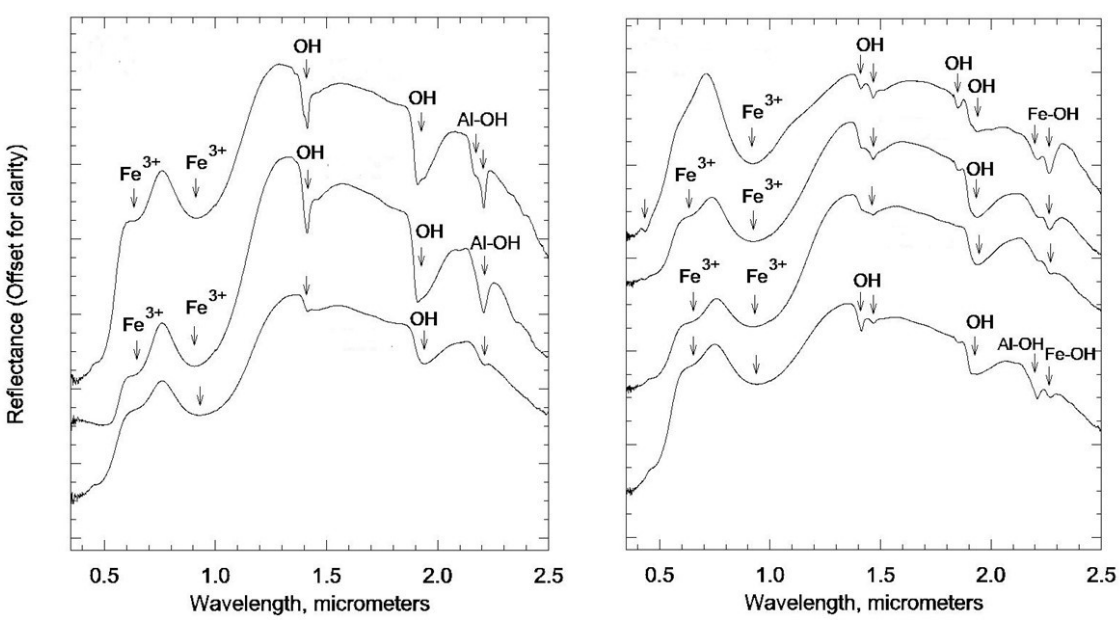

Figure 4. Several reflectance spectra of altered rock samples from the Kap Simpson study area.

Analysis of PRISMA data

The PRISMA image was processed using the Adaptive Coherence Estimator (ACE), a partial unmixing algorithm (e.g., Manolakis et al., 2016). The analysis of PRISMA hyperspectral image was focused in the wavelength regions where diagnostic absorption features of the main alteration minerals occur. The Adaptive Coherence Estimator is described as the squared matched filter normalized by terms proportional to the magnitude of the target in the matched filter space and the magnitude of the reference spectrum in the matched filter space (e.g., Schott, 2007). The reference spectra were derived from the hyperspectral image using the ‘‘hourglass” processing scheme (e.g., Kruse et al., 2006; Boardman and Kruse, 2011).

Results and discussion

The results of the Adaptive Coherence Estimator (ACE) analysis of the PRISMA hyperspectral image for the alteration minerals in the study area are shown in figure 5. The illite is related to the sedimentary lithology in the southern margins of the Kap Simpson complex, but also as an alteration product of the igneous rocks, spatially associated with zones of limonite and jarosite. The occurrence of kaolinite is related to zones of argillic alteration at Føndal. The hyperspectral data have identified widespread iron-stained zones consisting of limonite and jarosite. All these areas constitute prospection targets for the localization of economic mineralization including molybdenum, rare earth elements, gold, silver, and base metals. Intensive pyritization of the rocks correlates with the mapping of the mineral jarosite. Jarosite, an iron-sulfate mineral, is common in acidic, sulfate-rich environments formed by the oxidation of sulfides, especially pyrite (Baron and Palmer, 1996). At the Føndal area occur diffused pyrite to pyrite-hematite mineralization that in silicified zones reaches up to several weight per cent of the rock (CGRG, 2012).

In another setting, some 60 km south-west of the Kap Simpson complex, in the Werner Bjerge igneous complex, very close to a pyritizated zone is located the Malmbjerg world-class porphyry molybdenum deposit (Harpøth et al., 1986; Bedini, 2012). By analogy, the jarosite areas (shown in yellow color in figure 5) constitute prospection targets especially for porphyry molybdenum deposits. Lithogeochemical and stream sediment geochemistry investigations have shown Mo anomalies in these areas (e.g. Harpøth et al., 1986). From the perspective of the potential of the occurrence of significant accumulation of the Mo-porphyry type of mineralization, the most promising is the Føndal area (CGRG, 2012; figure 5). Rock samples from the Føndal area have Mo commonly between 5 to 50 ppm, less frequently above 100 ppm, whereas in two samples Mo contents higher than 1000 ppm have been recorded (CGRG, 2012).

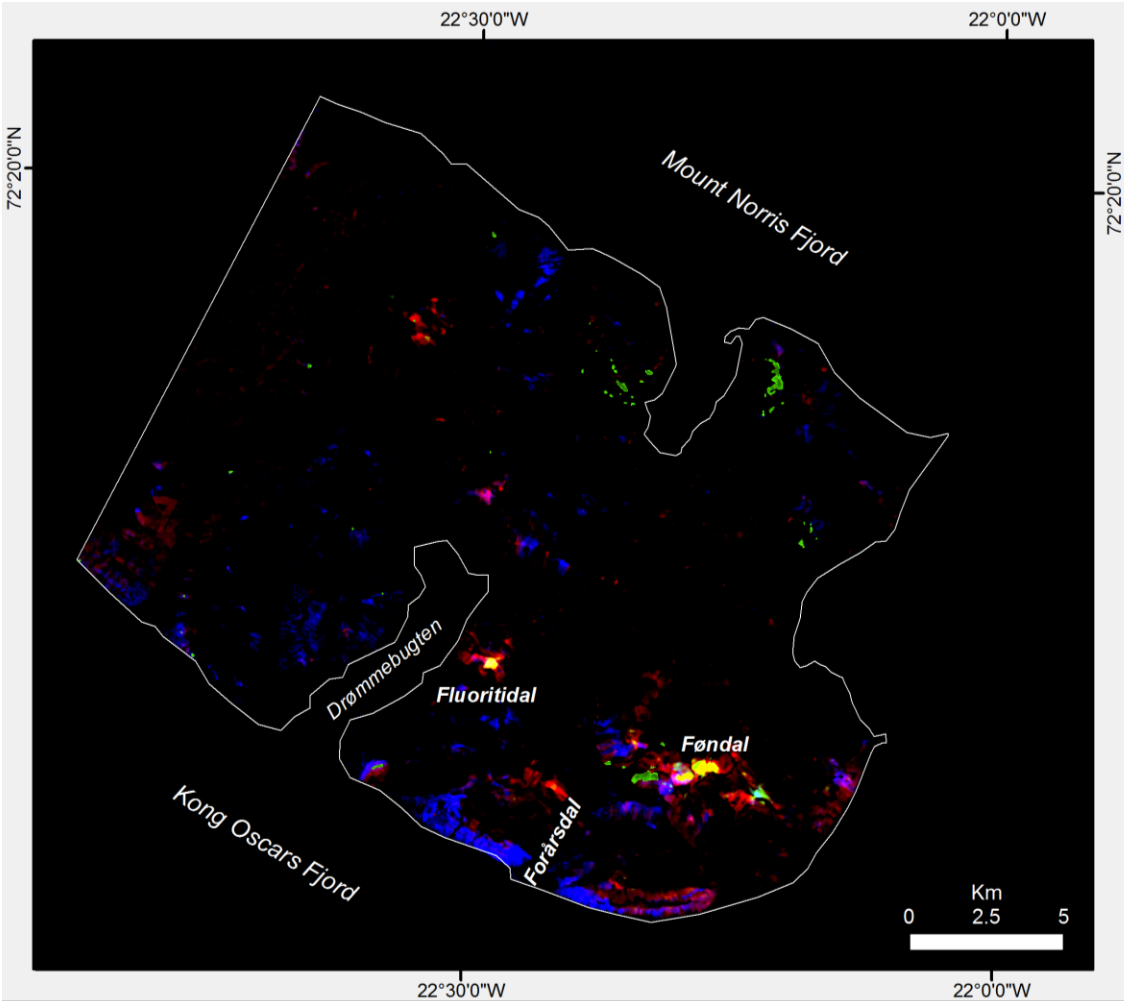

Figure 5. Results of the Adaptive Coherence Estimator (ACE) analysis of the PRISMA satellite hyperspectral imagery showing jarosite (in yellow color), limonite (in red color), illite (in blue color) and kaolinite (in green color).

Conclusions

Imagery recorded by the PRISMA hyperspectral imaging satellite of the Italian Space Agency was used to detect the zones of hydrothermal alteration in the Kap Simpson igneous rock complex in central East Greenland. The results bring new information for the iron stained areas in the igneous complex and the surrounding sedimentary units. The iron stained zones constitute prospection targets for a number of economic mineralizations. The zones distinguished by the spectral reflectance of the mineral jarosite correlate with intensively pyritizated areas and constitute prospection targets especially for molybdenum deposits. The PRISMA hyperspectral data have potential to provide useful information in the prospection for economic mineralization. On the other hand, the accurate mapping of surface mineralogy from hyperspectral data is also useful in geoenvironmental studies (e.g. Swayze et al. 2000).

Acknowledgment

The study was carried out using PRISMA Products, © of the Italian Space Agency (ASI), delivered under an ASI License to use. The Italian Space Agency is thanked for providing the PRISMA hyperspectral data.

References

Baron, D., and Palmer C.D., 1996. Solubility of jarosite at 4-35˚C. Geochimica et Cosmochimica Acta 60, 185-195.

Bedini, E. and Chen, J., 2020. Application of PRISMA satellite hyperspectral imagery to mineral alteration mapping at Cuprite, Nevada, USA. Journal of Hyperspectral Remote Sensing v, 10(2), 87-94.

Bedini, E., 2017. The use of hyperspectral remote sensing for mineral exploration: A review. Journal of Hyperspectral Remote Sensing, 7(4), 189-211.

Bedini, E., 2012. Mapping alteration minerals at Malmbjerg molybdenum deposit, central East Greenland, by Kohonen self-organizing maps and matched filter analysis of HyMap data. International Journal of Remote Sensing, 33(4), pp.939-961.

Bedini, E., 2011. Mineral mapping in the Kap Simpson complex, central East Greenland, using HyMap and ASTER remote sensing data. Advances in Space Research, 47, 60-73.

Bishop, J.L. and Murad, E., 2005. The visible and infrared spectral properties of jarosite and alunite. American Mineralogist 90, 1100–1107.

Boardman, J.W. and Kruse, F.A., 2011. Analysis of imaging spectrometer data using N-dimensional geometry and a mixture-tuned matched filtering approach. IEEE Trans. Geosci. Remote Sens. 49, 4138–4152.

Clark, R.N. Spectroscopy of Rocks and Minerals, and Principles of Spectroscopy, in: A. Rencz (Ed.), Manual of Remote Sensing vol. 3. Wiley and Sons Inc., New York, pp. 3-58, 1999.

CGRG, 2012. Exploration of the deposit potential of the Mo-Porphyry and Au-Epithermal types of mineralization within the framework of Minerals Special Exploration Licence No. 2011/51, on the Traill site in East Greenland. Report prepared by Lhotsky P., Broz B., Havranek J., Morysek J., Tvrdy J. (Report file 23636, GEUS-DODEX).

Conradsen, K. and Harpøth, O., 1984. Use of Landsat Multispectral Scanner Data for Detection and Reconnaissance Mapping of Iron Oxide Staining in Mineral Exploration, Central East Greenland. Economic Geology, 79, 1229-1244.

Damtoft, J.S. and Grahl-Madsen, L., 1982. Geological and VLF geophysical mapping of the Bredhorn Ba-Pb prospect and preliminary mapping on SE Traill Ø for porphyry molybdenum mineralization. Internal NM report 2/81, 118 p.

Geyti, A., 1979. Drilling and mapping in the EGMO concession area. Nordisk Minselskab prospecting report 13/1979, 44 p.

Harpøth, O., Pedersen J.L., Schønwandt H.K., Thomassen B., 1986. The mineral occurrences of central-east Greenland. Meddelelser om Grønland, Geoscience 17, 139 pp.

Heller Pearlshtien, D., Pignatti, S., Greisman-Ran, U. and Ben-Dor, E., 2021. PRISMA sensor evaluation: a case study of mineral mapping performance over Makhtesh Ramon, Israel. International Journal of Remote Sensing, 42, 5882-5914.

Kruse, F.A., Perry, S.L., Caballero, A., 2006. District-level mineral survey using airborne hyperspectral data, Los Menucos, Argentina. Annals of Geophysics 49, 83–92.

Manolakis, D., Lockwood, R., Cooley, T., 2016. Hyperspectral Imaging Remote Sensing: Physics, Sensors, and Algorithms. Cambridge University Press, p. 706 p.

Pignatti, S., Palombo, A., Pascucci, S., Romano, F., Santini, F., Simoniello, T., Umberto, A., Vincenzo, C., Acito, N., Diani, M., Matteoli, S., 2013. The PRISMA hyperspectral mission: Science activities and opportunities for agriculture and land monitoring. *In* 2013 IEEE International Geoscience and Remote Sensing Symposium-IGARSS, pp. 4558-4561, IEEE.

Schott, J.R., 2007. Remote Sensing. The Image Chain Approach, 2nd edition. Oxford University Press, New York, p. 688 p.

Swayze, G.A., Smith, K.S., Clark, R.N., Sutley, S.J., Pearson, R.M., Vance, J.S., Hageman, P.L., Briggs, P.H., Meier, A.L., Singleton, M.J. and Roth, S., 2000. Using imaging spectroscopy to map acidic mine waste. Environmental Science & Technology, 34, pp.47-54.

Tukiainen, T. and Thomassen, B., 2010. Application of airborne hyperspectral data to mineral exploration in North-East Greenland. GEUS Bulletin, 20, 71-74.

van der Meer, F.D., van der Werff, H.M., van Ruitenbeek, F.J., Hecker, C.A., Bakker, W.H., Noomen, M.F., van Der Meijde, M., Carranza, E.J.M., De Smeth, J.B., Woldai, T., 2012. Multi- and hyperspectral geologic remote sensing: A review. International Journal of Applied Earth Observation and Geoinformation, 14, 112-128.